AD-A115 814 WASHINGTON UNIV SEATTLE DEPT OF CHEMISTRY F/G 7/3
THE ISOMERIZATION OF 1-METHYL CYCLOBUTENE BY SINGLE COLLISION A--ETC(U)
JUN 82 R ARAKAWA, B S RABINOVITCH N00014-75-C-0690
UNCLASSIFIED TR-25 NL

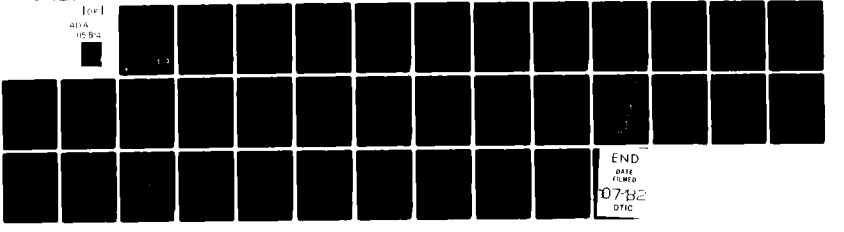

END
DATE FILMED
07-82
DTIC

(12)

The Isomerization of 1-Methyl Cyclobutene by Single Collision Activation at a Surface. Variation of Initial Energy.

by R. Arakawa and B. S. Rabinovitch

Department of Chemistry BG-10, University of Washington
Seattle, Washington 98195

Technical Report No. NR092-549-TR25

Contract N00014-75-C-0690, NR-092-549

June 1, 1982

Prepared for Publication in

Journal of Physical Chemistry

OFFICE OF NAVAL RESEARCH
Department of the Navy
Code 473
800 N. Quincy
Arlington, VA 22217

Unclassified

SECURITY CLASSIFICATION OF THIS PAGE (When Data Entered)

REPORT DOCUMENTATION PAGE		READ INSTRUCTIONS BEFORE COMPLETING FORM
1. REPORT NUMBER NR092-549-TR25	2. GOVT ACCESSION NO. A.D-A115 814	3. RECIPIENT'S CATALOG NUMBER
4. TITLE (and Subtitle) The Isomerization of 1-Methyl Cyclobutene by Single Collision Activation at a Surface. Variation of Initial Energy.		5. TYPE OF REPORT & PERIOD COVERED Technical 6. PERFORMING ORG. REPORT NUMBER
7. AUTHOR(s) R. Arakawa and B. S. Rabinovitch		8. CONTRACT OR GRANT NUMBER(s) N00014-75-C-0690 NR092-549
9. PERFORMING ORGANIZATION NAME AND ADDRESS Professor B. S. Rabinovitch Department of Chemistry BG-10 University of Washington Seattle, WA 98195		10. PROGRAM ELEMENT, PROJECT, TASK AREA & WORK UNIT NUMBERS
11. CONTROLLING OFFICE NAME AND ADDRESS Office of Naval Research, Code 743 Department of the Navy 800 N. Quincy Arlington, VA 22217		12. REPORT DATE June 1, 1982 13. NUMBER OF PAGES 27
14. MONITORING AGENCY NAME & ADDRESS(if different from Controlling Office)		15. SECURITY CLASS. (of this report) Unclassified 15a. DECLASSIFICATION/DOWNGRADING SCHEDULE

16. DISTRIBUTION STATEMENT (of this Report)

This document has been approved for public release; its distribution is unlimited.

17. DISTRIBUTION STATEMENT (of the abstract entered in Block 20, if different from Report)

Prepared for publication in J. Phys. Chem.

18. SUPPLEMENTARY NOTES

19. KEY WORDS (Continue on reverse side if necessary and identify by block number)

Accommodation coefficient
Cyclobutene
Energy Transfer
Gases
High Temperature
Methyl cyclobutene
Surfaces
Unimolecular Reaction
Vibrational Relaxation

20. ABSTRACT (Continue on reverse side if necessary and identify by block number)

The initial vibrational energy of molecules that collide with a hot surface has been varied. The effect on the collisional reaction probability (P_c) has been studied under single collision conditions. These experiments provide a sensitive test of the suitability of various analytical forms for the collisional transition probability matrix, P. The reaction system is the isomerization of methyl cyclobutene to pentadiene. A seasoned fused quartz surface was used over the temperature range T_r = 580 K - 800 K. Variation of the initial energy population vector of cyclobutene molecules was made by change of the initial temperature T_c in the range 273 K - 500 K. Gaussian forms of P prove to be the most suitable to fit the data.

DD FORM 1 JAN 73 1473 EDITION OF 1 NOV 65 IS OBSOLETE
S/N 0102 LF 014 6601

Unclassified

SECURITY CLASSIFICATION OF THIS PAGE (When Data Entered)

The Isomerization of 1-Methyl Cyclobutene by Single Collision Activation at a Surface. Variation of Initial Energy.*

by R. Arakawa# and B. S. Rabinovitch

Department of Chemistry BG-10, University of Washington

Seattle, Washington 98195

Abstract

The reaction probability per collision, P_c , for 1-methylcyclobutene activated at a hot seasoned fused silica surface has been measured under single collision conditions over the reactor temperature range T_r = 480 K - 800 K. The initial thermal vibrational energy population distribution of the cyclobutene molecules was varied from T_c = 273 K - 570 K. The reaction is isomerization to isoprene. Mixed samples of 1-methylcyclobutene and cyclobutene (which had been studied earlier) were used for internal comparison under the same conditions. These experiments provide a test of the relative suitability of various analytical forms for the collisional transition probability matrix $\underset{\sim}{P}$. Stochastic calculations with a Gaussian form provide the best overall fit to the data. The calculated average amount of energy ($\langle\Delta E'\rangle_{E_0}$) transferred from the hot molecules in a vibrational down transition from the reaction threshold energy level, E_0 , declined from 7220 cm^{-1} to 3890 cm^{-1} with increase in surface temperature from 600 K to 800 K. The experimental collisional efficiency, β_1 , declined from 0.39 to 0.035 over the combination temperature range T_r,T_c = 600,500 to 800,293. Strong collider behavior was observed with both 1-methyl cyclobutene and cyclobutene for T_r less than 450 K.

Introduction

Gas-surface vibrational energy accommodation is being intensively studied, both experimentally and theoretically.[1-5] The variable encounter method (VEM) provides a simple technique for the study of collisional transfer of vibrational energy between gas molecules and a surface [4,6-9] at levels of excitation corresponding to homogeneous unimolecular reaction. By this technique, cold substrate molecules that are initially equilibrated at low temperature T_c experience a known, and experimentally variable number of sequential collisions, m , with a hot reactor surface at temperature T_r before leaving the reactor and re-equilibrating to their initial low temperature. Values of m between 2 and 30 have been conventionally used. Gas molecules describe a random walk along an energy coordinate until they reach an absorbing level, the critical reaction threshold E_0, characteristic of the homogeneous gas reaction. Such relaxation of non-equilibrium vibrational energy distribution was described theoretically a number of years ago by Rubin and Shuler,[10] and by Kim[11] and Widom.[12]

Recently, single collision measurements (m = 1) by the VEM technique were described for the cyclobutene (CB) system.[13,14] Initial vibrational energy of CB was varied.[14] In the present communication, we have applied the single collision condition to the study of 1-methylcyclobutene (1-MCB) system for comparison with that of CB. The surface is a "seasoned" fused quartz finger. Although such a surface is not well defined, it is the conventional experimental surface of thermal kinetics.

The vibrational energy population vector of molecules after one collision, $\underset{\sim}{N}_1$, is given by $\underset{\sim}{N}_1 = \underset{\sim\sim}{P}\underset{\sim}{N}_c^{eq}$, where $\underset{\sim\sim}{P}$ is a collisional transition probability matrix, and $\underset{\sim}{N}_c^{eq}$ is the initial vibrational energy population vector that corresponds to the thermal Boltzmann distribution at the low temperature of the gas reservoir wall. Since no comprehensive theory of gas-surface collision interaction exists, at least for complex molecules on these surfaces, down-jump

transition probability elements of the $\underset{\sim}{P}$ matrix were constructed according to various assumed mathematical models; these have some plausible connections with physical reality. Up-jump transition probabilities were constructed from the down-jump transitions with use of the conditions of detailed balance and completeness.

The ring-opening unimolecular isomerization of 1-MCB to isoprene has a low E_0 (34.2 kcal mol^{-1}); that for CB is[15] 32.4 kcal $mole^{-1}$. The effect of the methyl substituent on the collisional reaction probability provides an interesting comparison. Previously, a similar comparison was made for the collisional relaxation of vibrational energy transients in the methyl cyclopropane and cyclopropane systems using a VEM(m > 1) technique.[9]

Experimental

The 1-MCB substrate sample was a mixture containing 14% of 3-MCB as impurity; it was not removed since it caused no complication and allowed a rough concurrent measurement for its own isomerization. A similar amount of cyclobutene was added as an internal standard. The reaction system apparatus used here was the same as that for previous single collision experiments.[13,14] The reaction vessel consisted of a 3-ℓ spherical pyrex reservoir flask that was provided with an internally heated, central fused-quartz finger. The flask and the finger were heated independently. Two experimental series were used to measure the isomerization rate constants: a) the surface temperature of the reactor finger was varied from 600 K to 800 K, while the wall temperature of the flask reservoir was varied from 273 K to 550 K. b) the reactor temperature was varied from 480 K to 800 K at constant wall temperature of 273 K. Temperature deviation of the finger surface was a maximum of ± 5°K at 800 K, and that of the flask wall was ± 10°K at 550 K. Before kinetic measurements were made, the reactive surface of fused quartz was "seasoned" at the highest temperature and the seasoning was maintained by exposure for a few hours to the mixture gas at a pressure of $\sim 5 \times 10^{-3}$ torr prior to each run.

The system was run in both static and flow modes in the pressure region between 10^{-4} and 10^{-3} torr, usually $\sim 2 \times 10^{-4}$ torr. For the flow mode, typical residence times in the reactor were 10 to 30 sec. Duration of a flow run was several minutes. Detailed description of both modes was given earlier.[13] Pressure measurements were made with an MKS 146H capacitance manometer.

Product analysis was performed by gas liquid phase chromatography on a 5 ft x 3/16 in. squalane column on Chromsorb P at 0°C with FID detection.

Results

Observed rate constants for 1-MCB isomerization to isoprene were calculated from the product yield. The total observed rate constant k_t was a sum of reaction due to heating at the reaction finger, k_r, and at the reservoir wall, k_c, given by

$$k_t(T_r,T_c) = k_r(T_r,T_c) + k_c(T_c)$$

Independent measurements of $k_c(T_c)$ were made under the experimental condition, $T_r = T_c$, with use of a minor area correction for the relative surface area of the reactor finger and the reservoir wall (1:13). Both rate constants k_t and k_c are shown in Fig. 1. Experimental values having a cross mark in Fig. 1 were rejected, since correction for k_c amounted to ≈ 50% of the total rate k_t. The reaction probability per collision, $P_c(T_r,T_c)$, was calculated from the finger surface reaction constant $k_r(T_r,T_c)$,

$$P_c(T_r,T_c) = k_r(T_r,T_c)/(A(8kT_c/\pi m)^{\frac{1}{2}}/4V) ,$$

where A is the reactor finger surface area, k is the Boltzmann constant, m is the molecular weight, and V is the volume of the reservoir flask. The values of the reaction probability are plotted as a function of T_c in Fig. 2 and are listed in Table 1. The experimental uncertainty in P_c is estimated to be ∿ 20%. Also listed is the collisional efficiency, β_1, defined as $\beta_1 = P_c(T_r,T_c)/P_c^{sc}(T_r)$; these quantities are the analog of the conventional[16] homogeneous thermal collisional efficiency factor, β. The values of $P_c^{sc}(T_r)$ are calculated from the Boltzmann distribution population vector characteristic of T_r.

The mathematical forms used here for the transition probability distribution of down-transition energy jumps ΔE are exponential (E), Gaussian (G), a Boltzmann weighted exponential (BE), and Gaussian (BG) functions, given by Eqs. (1)-(4):

$$p^{E}(\Delta E) = C_1 \exp(-\Delta E/\langle\Delta E\rangle) \quad (1)$$

$$p^{G}(\Delta E) = C_2 \exp(-(\Delta E-\Delta E_{mp})^2/2\sigma^2) \quad (2)$$

$$p^{BE}_{i\leftarrow j}(\Delta E) = C_3 B_i p^{E}(\Delta E) \quad (3)$$

$$p^{BG}_{i\leftarrow j}(\Delta E) = C_4 B_i p^{G}(\Delta E);\ B_i = g_i \exp(-E_i/RT_r) \quad (4)$$

Here, $\langle\Delta E\rangle$, ΔE_{mp}, and σ are parameters of the models, the C_i's are normalization constants; and B_i is a normalized Boltzmann distribution characteristic of the finger surface temperature, T_r, where g_i is the density of internal states at energy level E_i; σ is set equal to 0.7 ΔE_{mp} for the G and BG models. Transition probability values below E = 0 in a down transition from the energy level i were added to the element for elastic collisional transition probability, p_{ii}. The E and G models have been termed "flat"[6,7] since the distributions given by them are independent of the initial energy level. The microscopic rate constants at each reactive energy level were calculated by RRKM theory with use of the vibrational frequency assignment of Elliott and Frey;[15] these calculations were made with an energy grain size of 100 cm^{-1} that was also used to specify the transition probability matrix. Isomerization of excited molecules occurs during the average (collisionless) flight time between the reactor surface and the reservoir wall (9 cm). An average fraction, f_d, of molecules excited above E_0 that decompose during the flight time was calculated in order to estimate the dependence of the observed rate constant on the reaction probability. The most favorable experimental

situation is obtained for $f_d = 1$, corresponding to $k/k_\infty \to 0$ in a homogeneous system; in this case, which holds for CB, reaction is governed only by the collisionally activated population distribution, and the need for RRKM calculations of k(E), the specific reaction probability at internal energy E, with a postulated activated complex structure, is removed. In the present case, $f_d \sim 0.6\text{-}0.65$, so that the accuracy of the measurements was only moderately dependent on the accuracy of the RRKM calculational details. Clearly, as $f_d \to 0$, corresponding to $k/k_\infty \to 1$ in the $p \to \infty$ homogeneous case, no reliable information about energy transfer can be gained.

Results of the least squares fitting to the experimental P_c curve for each reaction surface temperature (with use of $\langle\Delta E\rangle$, or ΔE_{mp}, as the parameter of fit) are shown in Fig. 3 with use of four models. The corresponding parameters, the average down-transition energy $\langle\Delta E\rangle$ for E and BE, and the most probable energy ΔE_{mp} for G and BG, are listed in Table 2. We have chosen to exhibit, and use, these average values rather than to enumerate a plethora of best-fit values for each value of T_c for a given T_r. Obviously, use of an average constant parameter for the whole T_c range cannot give as good fit at each T_c as would an optimized value. The calculated value of $\langle\Delta E'\rangle_{E_0}$ is the average amount of energy transferred in a down-transition from the threshold energy level E_0; $\langle\Delta E'\rangle$ is independent of E_0 for E and G, but varies with initial level for BE and BG. Also listed is $\langle\Delta E^+\rangle_{av} = \left[\left(\bar{E}_f\right)_{E_f > E_0} - E_0\right]$, the average amount of energy transferred in an up transition to the levels above E_0. The average vibrational energy of 1-MCB molecules, $\bar{E}$, for the thermal Boltzmann distribution, is given for the temperatures of interest in Table 3. Another important quantity is the average energy transfer, ΔE_{av}, defined as $\Delta E_{av} = \bar{E}_f - \bar{E}_c$, where $\bar{E}_c$ and $\bar{E}_f$ are the average energies of molecules before and after single collision; ΔE_{av} is listed from results of E, G, and BE calculation in Table 4. The vibrational energy accommodation coefficient, α, is defined as $\alpha = \Delta E_{av}/(\bar{E}_r - \bar{E}_c)$, where $\bar{E}_r$ is the average energy $\bar{E}$ corresponding to $T = T_r$ and is given in Table 4.

Single collision experiments permit a more refined test of the correct form of $\underset{\sim}{P}$ than do m > 1 experiments. In particular, an even more stringent criterion is realized here by changing the initial population vector $\underset{\sim}{N}_c$. The features of the experimental P_c curves for all T_r in Fig. 2 are similar to those for CB and also exhibit a foot for T_c < 400 K. The best fits at higher temperatures were obtained with the E and G models. The BE and BG models fail to agree with the data curve. At lower temperature (T_r = 600 K) where collisional interaction becomes stronger, the E model cannot be fitted to the experimental curve of T_r = 600 K for any reasonable parameter of $\langle\Delta E\rangle$. For each model, Fig. 4 shows the normalized transition probability distribution $P_{i\leftarrow E_0}$ for up- and down-transitions from the level energy E_0 to the level i at a representative condition, T_r,T_c = 800, 400 for the parameters obtained by the least squares fitting.

It is of interest to examine the relative contribution of the various elements of $\underset{\sim}{N}_c$ to the vibrational activation to the level E_0 in $\underset{\sim}{N}_1$. The activation distribution, $p_{E_0\leftarrow i}n_{ci}$ vs E, is shown for the temperature combination (800,400) in Fig. 5 for the various model parameters fitted to experiment by least squares. The activation functions are mainly distributed around the initial energy 2000 cm^{-1}. The maxima would be shifted to higher energies if $\langle\Delta E'\rangle_{E_0}$ values were smaller as was illustrated previously[14] for CB.

The various transient population vectors $\underset{\sim}{N}_1$ that arise after single collision are shown in Fig. 6 for the E, G and BE models. For E and G, the $\underset{\sim}{N}_1$ population elements are distributed close to those for T_r = 800 K in the energy range below E = 10^4 cm^{-1}, while those for the BE model are much below the strong collider curve. The relative population in the energy range below E_0 provides the main criterion for the average amount of energy transferred on collision, ΔE_{av} and for the accommodation coefficient α. Thus, the BE model gives relatively small values of ΔE_{av} and α for the (Table 4). The same situation was found in the CB system.[14]

By contrast, P_c values are determined by the reacting state population

above E_0, in the $\underset{\sim}{N}_1$ vector, and which derives from the product of the up-transition probability to states above E_0 with the state populations of the $\underset{\sim}{N}_c$ vector below E_0. And although $\alpha(BE)$ is smaller than $\alpha(G)$ or $\alpha(E)$, it is evident from Fig. 6 that the BE model is relatively very efficient in transferring molecules to levels above E_0. Indeed, it gives rise to too-large values of P_c at higher temperatures. As discussed in our earlier CB study, the models for $\underset{\sim}{P}$ that fit the experimental P_c values are not necessarily adequate to predict α. It is clearly evident that measurements of α and of P_c are both desirable in order to deduce the most apt form of $\underset{\sim}{P}$.

Plots of $P_c(T_r,273)$ obtained by simultaneous measurements of gas mixtures containing both 1-MCB and CB are shown in Fig. 7. Filled squares represent the P_c values from the earlier CB experiment.[14] Good reproducibility for CB is evident and supports the presumption of a negligible role of catalytic reaction on the fused quartz surface.

Strong collider behavior is found for both CB and 1-MCB molecules curves at $T_r < 450$ K. This behavior for CB has been shown in earlier CB studies.[7,13,14] This trend is related to the fact that as T_r is lowered, the time that molecules spend trapped in the gas-surface potential well increases.

Some comparison of 1-MCB with CB for the single collision conditions are given in Table 6. The relatively larger experimental values of P_c for 1-MCB seems to result from the difference in molecular vibrational eigenstate densities, as illustrated by the mean vibrational energies at 400 K: 1-MCB, $\bar{E}_{400}$ = 1080 cm^{-1}; CB, $\bar{E}_{400}$ = 760 cm^{-1}.

The least squares fit values of $\langle \Delta E' \rangle_{E_0}$ for the G model, for 1-MCB and CB, are also listed in Table 6.

In the previous VEM studies ($m < 1$) of $P_c(T_r,273)$, comparison[9] of methylcyclopropane with cyclopropane and of[17] cyclopropane with cyclopropane-d_6 was

made with use of the best fitted E model in the reactor temperature range above T_r = 800 K. It was found that $\langle\Delta E'\rangle_{E_0}$ decreased with an increase in the vibrational heat capacity of each pair of molecules. The energy transfer (m = 1) parameters for 1-MCB and CB fitted to the experimental $P_c(T_r, 273)$ values are listed with use of the G model in Table 6. The more complex 1-MCB molecule appears to exhibit somewhat stronger collider behavior, unlike the methyl- and the cyclopropane systems where the smaller molecule gave larger $\langle\Delta E'\rangle$ values. The same trend is observed in the $\langle\Delta E'\rangle_{E_0}$ values calculated with use of the best fit E model to the T_r = 800 curve, and in the collisional efficiency β_1. We must leave this effect of structure for future resolution.

The G model leads to $\alpha \sim 0.9$-1.0 for all T_r used (Table 4).

Acknowledgment: We thank Professor H. M. Frey for the gift of a sample of 1-MCB. This work was supported by the Office of Naval Research.

Table 1. Experimental reaction probability per collision and collisional efficiencies in 1-methyl cyclobutene system.

T_r \ T_c		273	400	500	550
800	P_c	2.8×10^{-4}	3.1×10^{-4}	4.5×10^{-4}	5.5×10^{-4}
	β_1[a]	0.035	0.039	0.056	0.068
700	P_c	7.0×10^{-5}	8.0×10^{-5}	1.2×10^{-4}	
	β_1	0.081	0.092	0.138	
600	P_c	6.5×10^{-6}	8.6×10^{-6}	1.25×10^{-5}	
	β_1	0.201	0.265	0.386	

a) Collisional efficiency β_1 defined as $\beta_1 = P_c(T_r,T_c)/P_c^{sc}(T_r)$, where $P_c^{sc}(T_r)$ is the reaction probability for strong collider interaction of the molecule with the surface.

Table 2. Energy transfer parameters[a] for E, G, BE, and BG models obtained by least square fitting in 1-methyl cyclobutene system.

T_r(K)	Model	$\langle\Delta E\rangle$ or ΔE_{mp}	$\langle\Delta E'\rangle_{E_0}$	ΔE^+_{av}
800		3280	2850[c]	890
700	E	5820	3650[c]	800
600		---[b]	---	---
800		3890	4300[c]	630
700	G	4800	5180[c]	580
600		7220	6430[c]	580
800		1790	3440	1130
700	BE	1730	4780	910
600		1770	6850	690
800		3570	5210	500
700	BG	3570	6290	500
600		4160	7780	500

a) The energy unit is cm^{-1}

b) The E model could not be fitted to the 600 K curve in Fig. 3.

c) Differ from column 3 due to truncation effects

Table 3. Average energy of the thermal Boltzmann population in 1-methyl cyclobutene system.

T(K)	273	400	500	600	700	800
$\bar{E}(cm^{-1})$	410	1080	1870	2860	4030	5320

Table 4. Average energy transfer ΔE_{av}[a] and vibrational energy accommodation coefficient α[b] for 1-methyl cyclobutene by single collision with a seasoned fused quartz surface.

Tr(K)	Model	273	400	500	550
800		4910, 0.94	3630, 0.86	2600, 0.75	2090, 0.70
700	E	3460, 0.96	2470, 0.84	1540, 0.72	--
600		--	--	--	
800		4670, 0.95	3950, 0.93	3120, 0.91	2640, 0.89
700	G	3580, 0.99	2870, 0.97	2030, 0.94	--
600		2440, 1.0	1720, 0.96	910, 0.92	--
800		990, 0.20	960, 0.23	860, 0.25	780, 0.26
700	BE	960, 0.27	860, 0.29	690, 0.32	
600		920, 0.38	730, 0.41	440, 0.45	

a) $\Delta E_{av} = \bar{E}_f - \bar{E}_c$ (cm^{-1})

b) $\alpha = \Delta E_{av}/(\bar{E}_r - \bar{E}_c)$

Table 5. Some comparisons of 1-methyl cyclobutene with cyclobutene in single collision systems.

	CB[14]	1-MCB[a]
$P_c(800, 400)$	4×10^{-5}	3×10^{-4}
$P_c(600, 400)$	1×10^{-6}	9×10^{-6}
E_0(kcal mole^{-1})	32.4	34.2
k(E) (sec^{-1})[b]	$\sim 10^5$	$\sim 10^3$
f_d	1	0.64(800,500)[e]
		0.60(600, 273)[e]
$\bar{E}_{400}$(cm^{-1})[c]	760	1080
$\langle\Delta E'\rangle_{E_0}$[d]	4090	4300

a) Present work

b) The isomerization rate constant by RRKM theory at several 100 cm^{-1} above E_0.

c) Average thermal energy at 400 K.

d) Average down transition energy from the level of energy E_0, given by the G model for T_r = 800 K.

e) Calculated by G model.

Table 6. Energy transfer parameters[a] fitted to experimental $P_c(T_t,273)$ with the G model in the 1-MCB and CB systems.

T_r(K)		600	700	800
$\langle\Delta E'\rangle_{E_0}$	CB	5595	4580	4070 (2490)[b]
	1-MCB	6325	5350	4630 (2870)[b]
ΔE_{av}	CB	1620	2420	3200 (2480)[b]
	1-MCB	2440	3590(3450)[b]	4740 (4640)[b]
α	CB	0.96	0.96	0.94 (0.73)[b]
	1-MCB	1.0	0.97(0.96)[b]	0.97 (0.95)[b]
β_1	CB	0.13	0.044	0.021
	1-MCB	0.21	0.084	0.036

a) In units of cm^{-1}

b) Parenthetic calculation made with the least squares fitted E model.

References

* Work supported by the Office of Naval Research.

Permanent address: Dept. of Chemistry, Osaka University, Osaka 560, Japan

1. Goodman, F. O.; Wachman, H. Y. "Dynamics of Gas Surface Scattering", Academic Press, New York, 1976.
2. Draper, C. W.; Rosenblatt, G. M. J. Chem. Phys. 1978, 69, 1465; Foner, S. N.; Hudson, R. L. J. Chem. Phys. 1981, 75, 4727.
3. Prada-Silva, G.; Löffler, O.; Halpern, B. L.; Haller, G. L.; Fenn, J. B. Surface Sci. 1979, 83, 453.
4. Kelley, D. F.; Barton, B. D.; Zalotai, L.; Rabinovitch, B. S. J. Chem. Phys. 1979, 71, 358; Kelley, D. F.; Zalotai, L.; Rabinovitch, B. S. Chem. Phys. 1980, 46, 379.
5. Connolly, M. S.; Greene, E. F.; Gupta, C.; Marzuk, P.; Morton, T. H.; Parks, C.; Staker, G. J. Phys. Chem. 1981, 85, 235.
6. Flowers, M. C.; Wolters, F. C.; Barton, B. D.; Rabinovitch, B. S. Chem. Phys. 1980, 47, 189.
7. Flowers, M. C.; Wolters, F. C.; Kelley, D. F.; Rabinovitch, B. S. Chem. Phys. Lett. 1980, 69, 543.
8. Wolters, F. C.; Flowers, M. C.; Rabinovitch, B. S. J. Phys. Chem. 1981, 85, 589.
9. Kelley, D. F.; Kasai, T.; Rabinovitch, B. S. J. Chem. Phys. 1980, 73, 5611.
10. Rubin, R. J.; Shuler, K. E. J. Chem. Phys. 1956, 25, 59,68 et seq.
11. Kim, S. K. J. Chem. Phys. 1958, 28, 1057.
12. Widom, B. J. Chem. Phys. 1959, 31, 1387; 1961, 34, 2050.
13. Kelley, D. F.; Kasai, T.; Rabinovitch, B. S. J. Phys. Chem. 1981, 85, 1100.
14. Arakawa, R.; Kelley, D. F.; Rabinovitch, B. S. J. Chem. Phys. 1982, 76, 2384.

15. Elliot, C. S.; Frey, H. M. Trans. Far. Soc. 1966, 62, 895.

16. Tardy, D. C.; Rabinovitch, B. S. Chem. Revs. 1977, 77, 369.

17. Yuan, W.; Tosa, R.; Chao, K.-J.; Rabinovitch, B. S. Chem. Phys. Lett. 1982, 85, 27.

Figure Captions

Fig. 1. Observed isomerization rate constants of 1-methylcyclobutene to isoprene. Open and solid points represent the total rate constants, k_t, and the wall collisional rate constants, k_c. The crossed points were not used for the P_c calculations.

Fig. 2. Plot of P_c verus the initial temperature T_c.

Fig. 3. Calculated $P_c(T_r,T_c)$ plots for each finger surface temperature by least square fitting with use of the E (— -- —), G (— - — -), BE (------), and BG (—— —— ——) models; the heavy solid line summarizes the experimental curve.

Fig. 4. Plot of normalized transition probability distributions for down and up jumps starting from the vibrational energy level E_0 = 11950 cm^{-1}, calculated for the E, G, BE, and BG models for the temperature combination T_r, T_c = 800, 400.

Fig. 5. Curves showing relative contribution of the various elements of $\underset{\sim}{N}_c$ to vibrational activation to the level E_0 in $\underset{\sim}{N}_1$, given by $P_{E_0 \leftarrow i} n_{ci}$. These illustrative plots were calculated for the reaction temperature combination (800,400) on the basis of the least squares fitted parameters and are plotted with arbitrary units of the ordinate. Obviously, slightly different curves would result from a different temperature combination or different fitting procedure.

Fig. 6 Relative population distribution vector versus energy E. $\underset{\sim}{N}_c^{eq}$ and $\underset{\sim}{N}_r^{eq}$ represent the Boltzmann distribution curves characteristic of the initial temperature, T_c = 400 K, and the reactor surface temperature, T_r = 800 K, respectively. $\underset{\sim}{N}_1$ superscripted E, G, and BE represent the transient distribution curve after one collision with the surface, the two left ordinates apply. The k(E) curve is the RRKM isomerization rate constant to which the right side ordinate applies.

Fig. 7 Plots of experimental values of $P_c(T_r,273)$ versus T_r for 1-MCB (——) and CB (----) substrates measured by internal comparison in the same conditional reaction system. Also shown are the calculated strong-collider $P_c^{sc}(T_r)$ curve. Solid squares represent earlier experimental values.[14]

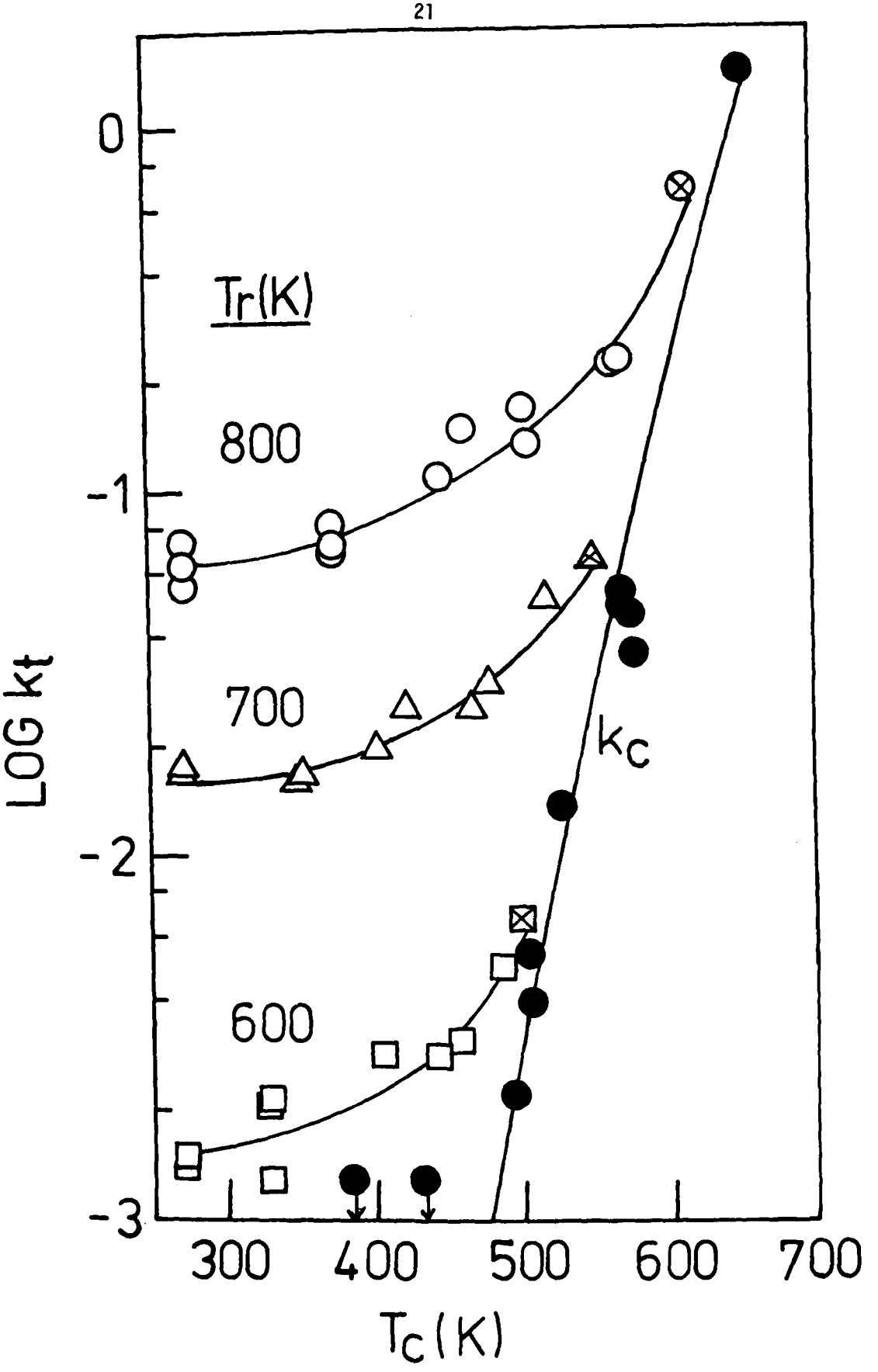

Fig. 1

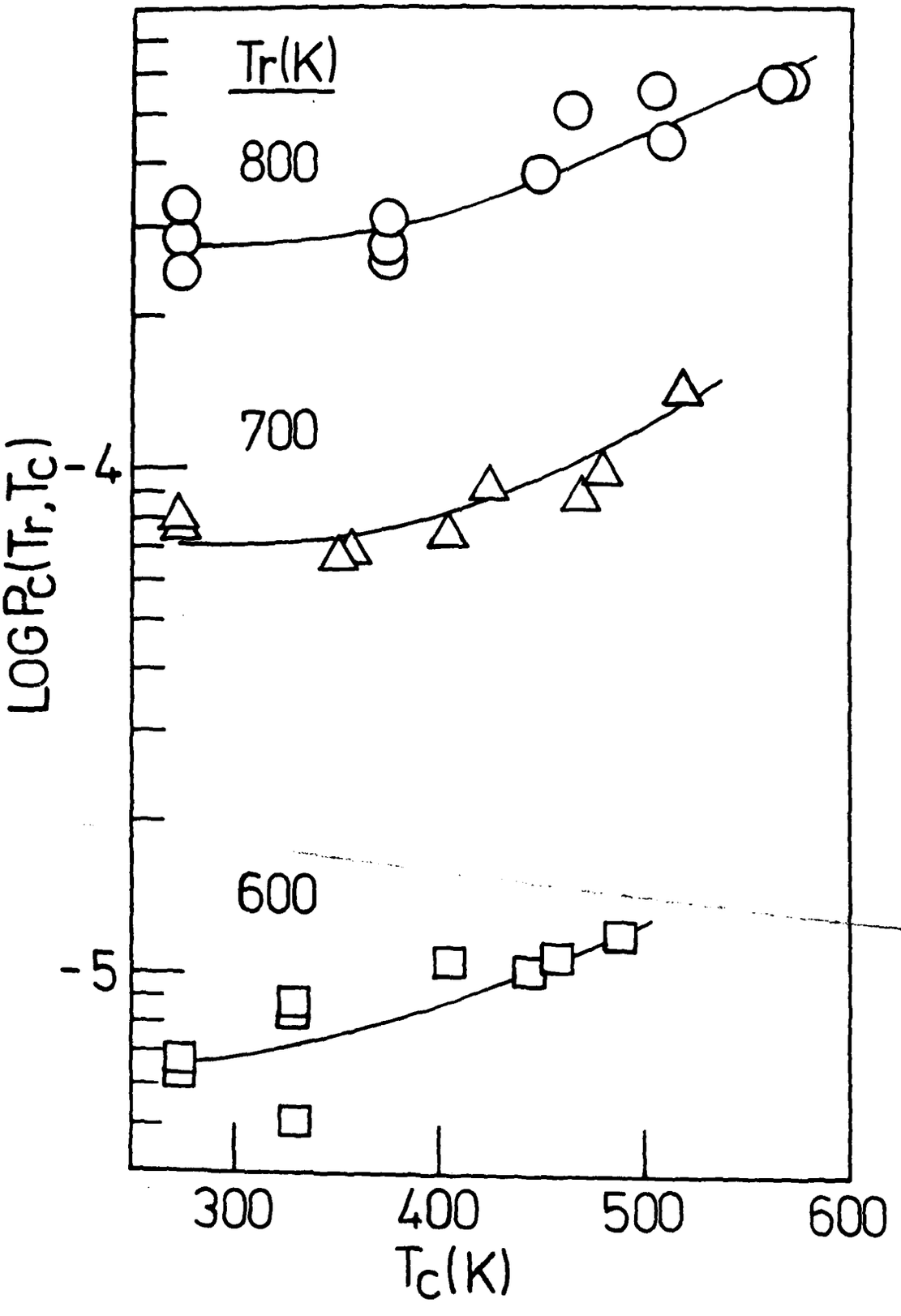
Tr(K)
800
700
600
LOG Pc(Tr, Tc)
-4
-5
300
400
500
600
Tc(K)

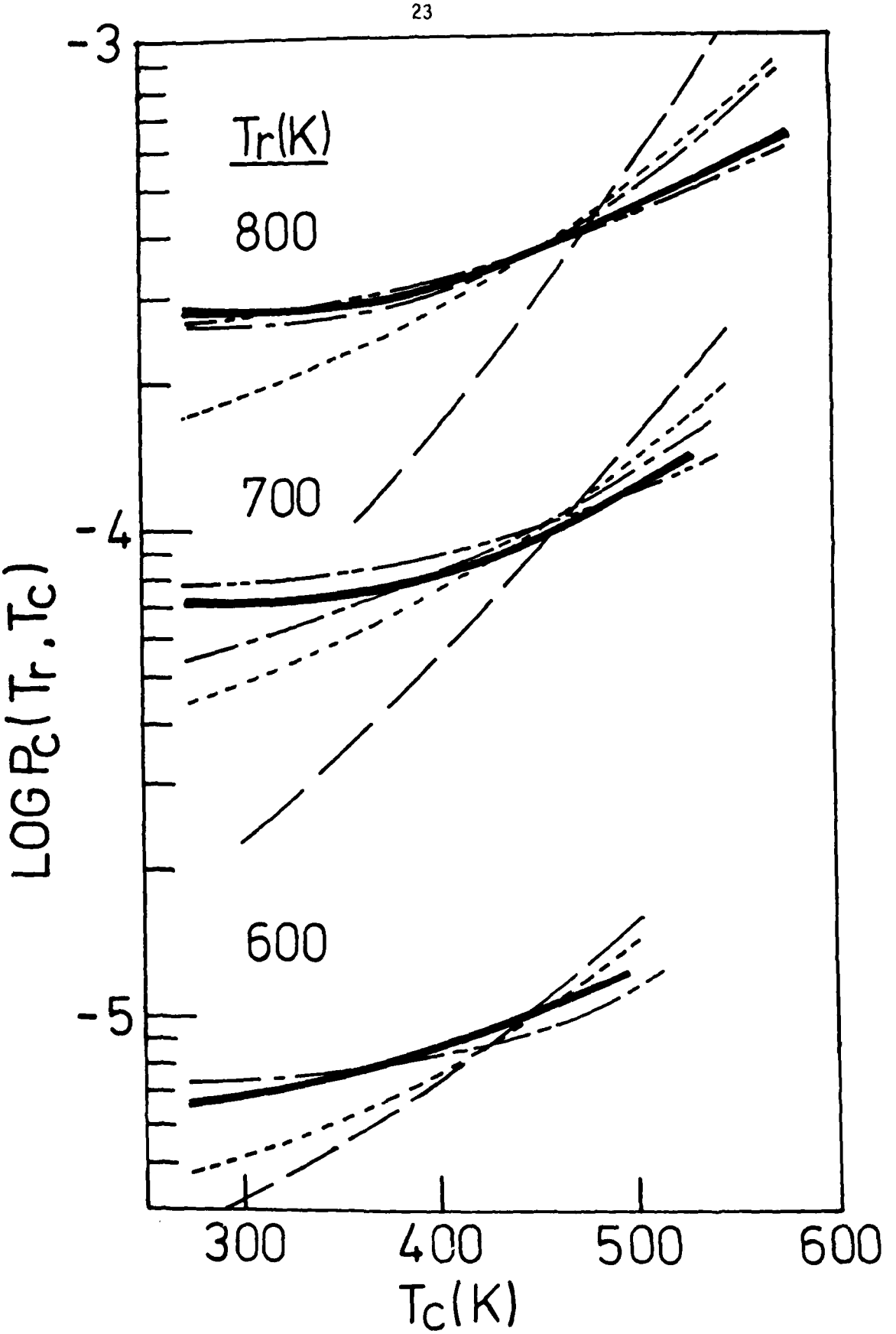
-3
-4
-5
Tr(K)
800
700
600
LOG Pc(Tr, Tc)
300
400
500
600
Tc(K)

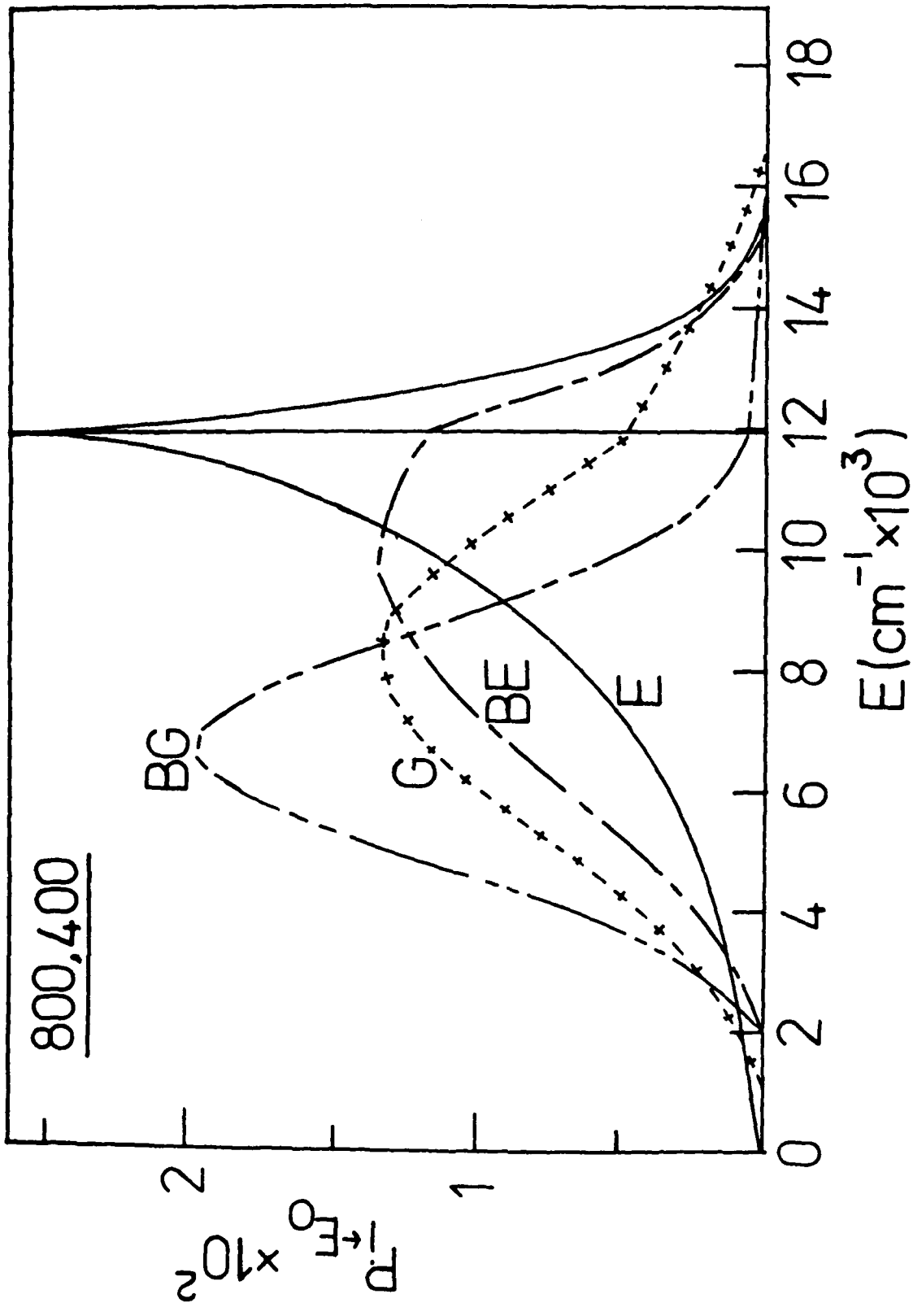
800,400
BG
G
BE
E
$P_{i\to E_0} \times 10^2$
$E(cm^{-1} \times 10^3)$
0
2
4
6
8
10
12
14
16
18
1
2

Fig. 4

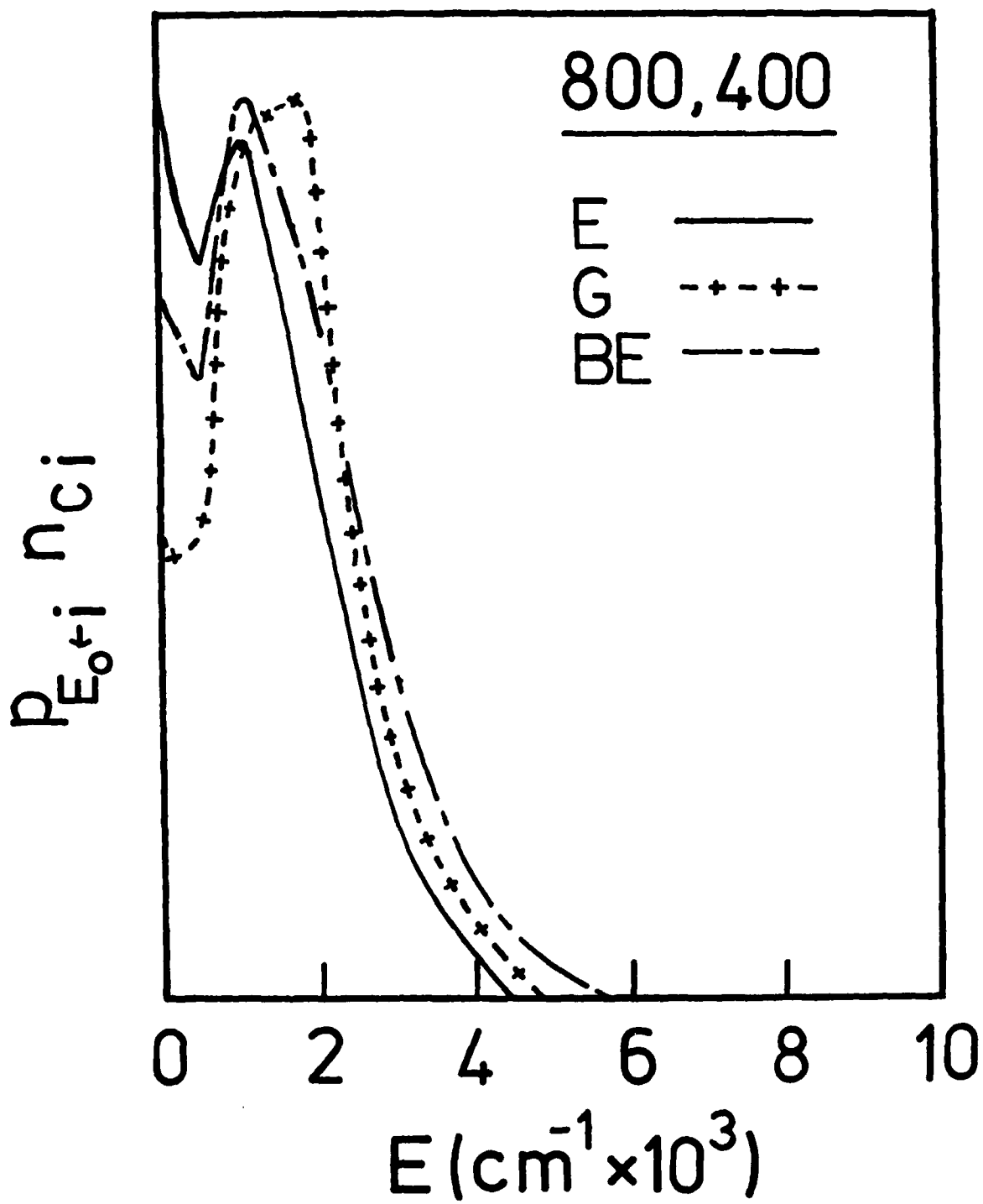

7/15

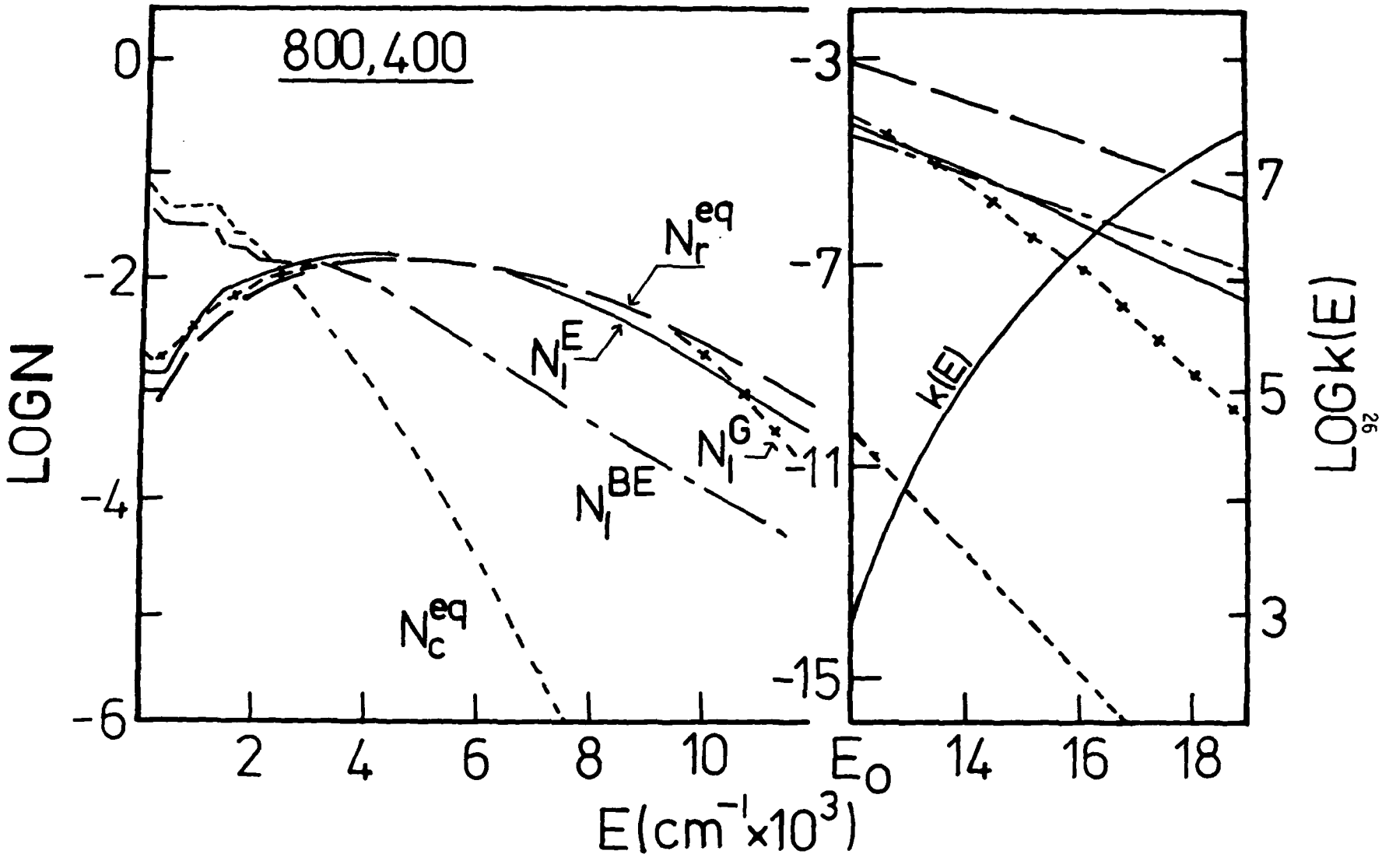
800,400
LOGN
0
-2
-4
-6
-3
-7
-11
-15
7
5
3
LOGK(E)
N_r^{eq}
N_l^E
N_l^G
N_l^{BE}
N_c^{eq}
k(E)
2
4
6
8
10
E_0
14
16
18
$E(cm^{-1}\times10^3)$

Fig. 6

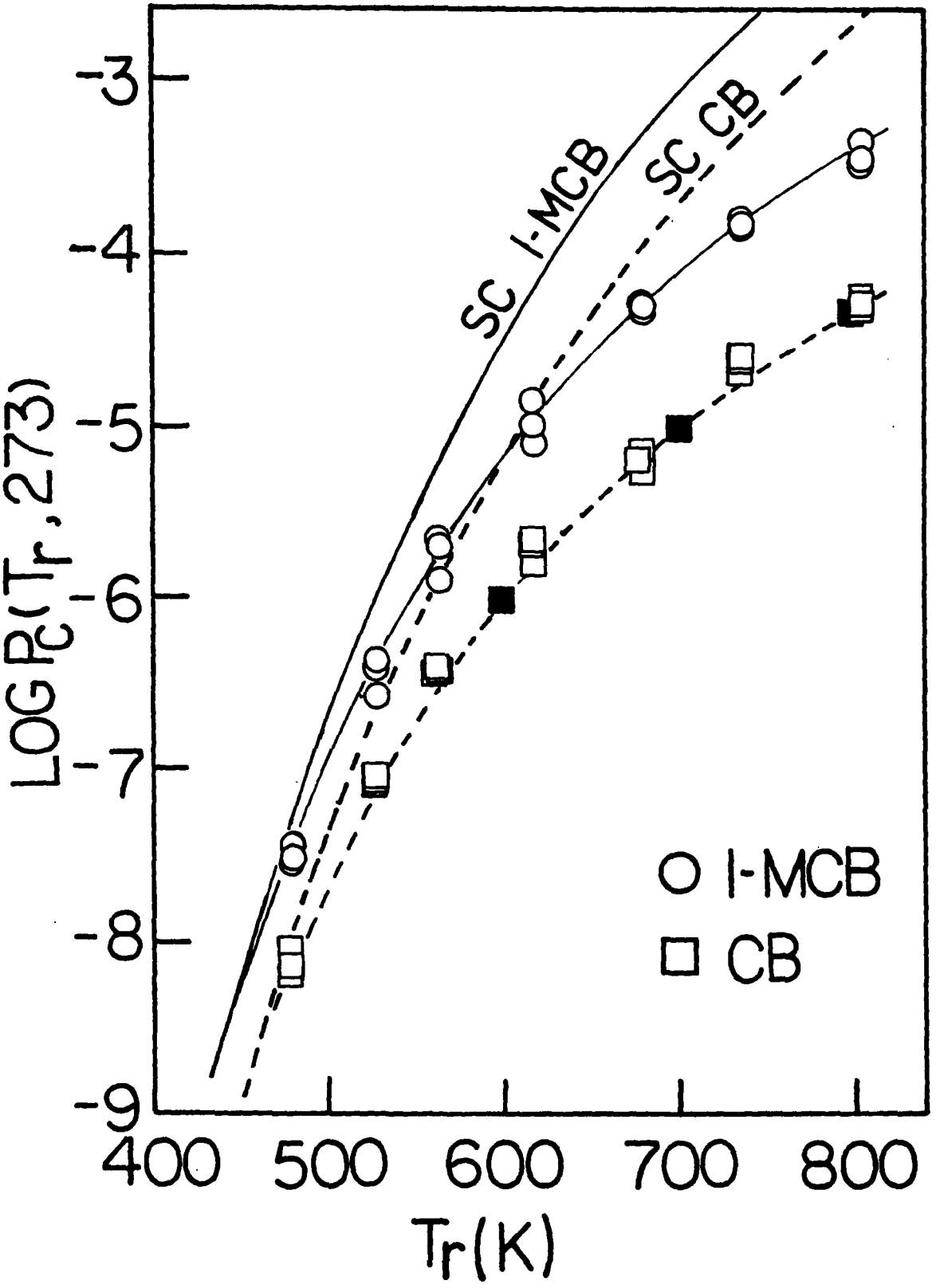
SC 1-MCB
SC CB
O 1-MCB
□ CB
LOG Rc(Tr, 273)
-3
-4
-5
-6
-7
-8
-9
400
500
600
700
800
Tr(K)

INIT

DISTRIBUTION LIST

June 1, 1982

	No. Copies
Dr. L.V. Schmidt Assistant Secretary of the Navy (R,E, and S) Room 5E 731 Pentagon Washington, D.C. 20350	1
Dr. A.L. Slafkosky Scientific Advisor Commandant of the Marine Corps Code RD-1 Washington, D.C. 20380	
Dr. Richard S. Miller Office of Naval Research Code 473 Arlington, VA 22217	10
Mr. David Siegel Office of Naval Research Code 260 Arlington, VA 22217	1
Dr. R.J. Marcus Office of Naval Research Western Office 1030 East Green Street Pasadena, CA 91106	1
Dr. Larry Peebles Office of Naval Research East Central Regional Office 666 Summer Street, Bldg. 114-D Boston, MA 02210	1
Dr. Phillip A. Miller Office of Naval Research San Francisco Area Office One Hallidie Plaza, Suite 601 San Francisco, CA 94102	1
Mr. Otto K. Heiney AFATL - DLDL Eglin AFB, FL 32542	1
Mr. R. Geisler ATTN: MKP/MS24 AFRPL Edwards AFB, CA 93523	1
Dr. F. Roberto Code AFRPL MKPA Edwards AFB, CA 93523	1
Dr. L.H. Caveny Air Force Office of Scientific Research Directorate of Aerospace Sciences Bolling Air Force Base Washington, D.C. 20332	1
Mr. Donald L. Ball Air Force Office of Scientific Research Directorate of Chemical Sciences Bolling Air Force Base Washington, D.C. 20332	1
Dr. John S. Wilkes, Jr. FJSRL/NC USAF Academy, CO 80840	1
Dr. R.L. Lou Aerojet Strategic Propulsion Co. P.O. Box 15699C Sacramento, CA 95813	1
Dr. V.J. Keenan Anal-Syn Lab Inc. P.O. Box 547 Paoli, PA 19301	1
Dr. Philip Howe Army Ballistic Research Labs ARRADCOM Code DRDAR-BLT Aberdeen Proving Ground, MD 21005	1
Mr. L.A. Watermeier Army Ballistic Research Labs ARRADCOM Code DRDAR-BLI Aberdeen Proving Ground, MD 21005	1
Dr. W.W. Wharton Attn: DRSMI-RKL Commander U.S. Army Missile Command Redstone Arsenal, AL 35898	1

INIT

DISTRIBUTION LIST

	No. Copies
Mr. J. Murrin Naval Sea Systems Command Code 62R2 Washington, D.C. 20362	1
Dr. P.J. Pastine Naval Surface Weapons Center Code R04 White Oak Silver Spring, MD 20910	1
Mr. L. Roslund Naval Surface Weapons Center Code R122 White Oak Silver Spring, MD 20910	1
Mr. M. Stosz Naval Surface Weapons Center Code R121 White Oak Silver Spring, MD 20910	1
Dr. E. Zimmet Naval Surface Weapons Center Code R13 White Oak Silver Spring, MD 20910	1
Dr. D.R. Derr Naval Weapons Center Code 388 China Lake, CA 93555	1
Mr. Lee N. Gilbert Naval Weapons Center Code 3205 China Lake, CA 93555	1
Dr. E. Martin Naval Weapons Center Code 3858 China Lake, CA 93555	1
Mr. R. McCarten Naval Weapons Center Code 3272 China Lake, CA 93555	1
Dr. A. Nielsen Naval Weapons Center Code 385 China Lake, CA 93555	1
Dr. R. Reed, Jr. Naval Weapons Center Code 388 China Lake, CA 93555	1
Dr. L. Smith Naval Weapons Center Code 3205 China Lake, CA 93555	1
Dr. B. Douda Naval Weapons Support Center Code 5042 Crane, IN 47522	1
Dr. A. Faulstich Chief of Naval Technology MAT Code 0716 Washington, D.C. 20360	1
LCDR J. Walker Chief of Naval Material Office of Naval Technology MAT, Code 0712 Washington, D.C. 20360	1
Mr. Joe McCartney Naval Ocean Systems Center San Diego, CA 92152	1
Dr. S. Yamamoto Marine Sciences Division Naval Ocean Systems Center San Diego, CA 91232	1
Dr. G. Bosmajian Applied Chemistry Division Naval Ship Research & Development Center Annapolis, MD 21401	1
Dr. H. Shuey Rohm and Haas Company Huntsville, AL 35801	1

INIT

DISTRIBUTION LIST

	No. Copies
Mr. R. Brown Naval Air Systems Command Code 330 Washington, D.C. 20361	1
Dr. H. Rosenwasser Naval Air Systems Command AIR-310C Washington, D.C. 20360	1
Mr. B. Sobers Naval Air Systems Command Code 03P25 Washington, D.C. 20360	1
Dr. L.R. Rothstein Assistant Director Naval Explosives Dev. Engineering Dept. Naval Weapons Station Yorktown, VA 23691	1
Dr. Lionel Dickinson Naval Explosive Ordnance Disposal Tech. Center Code D Indian Head, MD 20640	1
Mr. C.L. Adams Naval Ordnance Station Code PM4 Indian Head, MD 20640	1
Mr. S. Mitchell Naval Ordnance Station Code 5253 Indian Head, MD 20640	1
Dr. William Tolles Dean of Research Naval Postgraduate School Monterey, CA 93940	1
Naval Research Lab. Code 6100 Washington, D.C. 20375	1
Dr. J. Schnur Naval Research Lab. Code 6510 Washington, D.C. 20375	1
Mr. R. Beauregard Naval Sea Systems Command SEA 64E Washington, D.C. 20362	1
Mr. G. Edwards Naval Sea Systems Command Code 62R3 Washington, D.C. 20362	1
Mr. John Boyle Materials Branch Naval Ship Engineering Center Philadelphia, PA 19112	1
Dr. H.G. Adolph Naval Surface Weapons Center Code R11 White Oak Silver Spring, MD 20910	1
Dr. T.D. Austin Naval Surface Weapons Center Code R16 Indian Head, MD 20640	1
Dr. T. Hall Code R-11 Naval Surface Weapons Center White Oak Laboratory Silver Spring, MD 20910	1
Mr. G.L. Mackenzie Naval Surface Weapons Center Code R101 Indian Head, MD 20640	1
Dr. K.F. Mueller Naval Surface Weapons Center Code R11 White Oak Silver Spring, MD 20910	1

DISTRIBUTION LIST

	No. Copies
Dr. R.G. Rhoades Commander Army Missile Command DRSMI-R Redstone Arsenal, AL 35898	1
Dr. W.D. Stephens Atlantic Research Corp. Pine Ridge Plant 7511 Wellington Rd. Gainesville, VA 22065	1
Dr. A.W. Barrows Ballistic Research Laboratory USA ARRADCOM DRDAR-BLP Aberdeen Proving Ground, MD 21005	1
Dr. C.M. Frey Chemical Systems Division P.O. Box 358 Sunnyvale, CA 94086	1
Professor F. Rodriguez Cornell University School of Chemical Engineering Olin Hall Ithaca, NY 14853	1
Defense Technical Information Center DTIC-DDA-2 Cameron Station Alexandria, VA 22314	12
Dr. Rocco C. Musso Hercules Aerospace Division Hercules Incorporated Alleghany Ballistic Lab P.O. Box 210 Washington, DC 21502	1
Dr. Ronald L. Simmons Hercules Inc. Eglin AFATL/DLDL Eglin AFB, FL 32542	1
Dr. E.H. Debutts Hercules Inc. Baccus Works P.O. Box 98 Magna, UT 84044	1
Dr. James H. Thacher Hercules Inc. Magna Baccus Works P.O. Box 98 Magna, UT 84044	1
Mr. Theodore M. Gilliland Johns Hopkins University APL Chemical Propulsion Info. Agency Johns Hopkins Road Laurel, MD 20810	1
Dr. R. McGuire Lawrence Livermore Laboratory University of California Code L-324 Livermore, CA 94550	1
Dr. Jack Linsk Lockheed Missiles & Space Co. P.O. Box 504 Code Org. 83-10, Bldg. 154 Sunnyvale, CA 94088	1
Dr. B.G. Craig Los Alamos National Lab P.O. Box 1663 NSP/DOD, MS-245 Los Alamos, NM 87545	1
Dr. R.L. Rabie WX-2, MS-952 Los Alamos National Lab. P.O. Box 1663 Los Alamos, NM 87545	1
Dr. R. Rogers Los Alamos Scientific Lab. WX-2 P.O. Box 1663 Los Alamos, NM 87545	1

6/81

DISTRIBUTION LIST

	No. Copies
Dr. J.F. Kincaid Strategic Systems Project Office Department of the Navy Room 901 Washington, D.C. 20376	1
Strategic Systems Project Office Propulsion Unit Code SP2731 Department of the Navy Washington, D.C. 20376	1
Mr. E.L. Throckmorton Strategic Systems Project Office Department of the Navy Room 1048 Washington, D.C. 20376	1
Dr. D.A. Flanigan Thiokol Huntsville Division Huntsville, AL 35807	1
Mr. G.F. Mangum Thiokol Corporation Huntsville Division Huntsville, AL 35807	1
Mr. E.S. Sutton Thiokol Corporation Elkton Division P.O. Box 241 Elkton, MD 21921	1
Dr. G. Thompson Thiokol Wasatch Division MS 240 P.O. Box 524 Brigham City, UT 84302	1
Dr. T.F. Davidson Technical Director Thiokol Corporation Government Systems Group P.O. Box 9258 Ogden, UT 84409	1
Dr. C.W. Vriesen Thiokol Elkton Division P.O. Box 241 Elkton, MD 21921	1
Dr. J.C. Hinshaw Thiokol Wasatch Division P.O. Box 524 Brigham City, UT 83402	1
U.S. Army Research Office Chemical & Biological Sciences Division P.O. Box 12211 Research Triangle Park, NC 27709	1
Dr. R.F. Walker USA ARRADCOM DRDAR-LCE Dover, NJ 07801	1
Dr. T. Sinden Munitions Directorate Propellants and Explosives Defense Equipment Staff British Embassy 3100 Massachusetts Ave. Washington, D.C. 20008	1
Mr. J.M. Frankle Army Ballistic Research Labs ARRADCOM Code DRDAR-BLI Aberdeen Proving Ground, MD 21005	1
Dr. Ingo W. May Army Ballistic Research Lab ARRADCOM Code DRDAR-BLI Aberdeen Proving Ground, MD 21005	1

DISTRIBUTION LIST

No. Copies

E. J. Palm 1
Commander
Army Missile Command
DRSMI-RK
Redstone Arsenal, AL 35898

Dr. Merrill K. King 1
Atlantic Research Corp.
5390 Cherokee Avenue
Alexandria, VA 22314

Dr. R.J. Bartlett 1
Batelle Columbus Laboratories
505 King Avenue
Columbus, OH 43201

Dr. P. Rentzepis 1
Bell Laboratories
Murray Hill, NJ 07971

Professor Y.T. Lee 1
Department of Chemistry
University of California
Berkeley, CA 94720

Professor M. Nicol 1
Department of Chemistry
405 Hilgard Avenue
University of California
Los Angeles, CA 90024

Professor S.S. Penner 1
University of California
Energy Center
Mail Code B-010
La Jolla, CA 92093

Professor Curt Wittig 1
University of Southern CA
Dept. of Electrical Engineering
University Park
Los Angeles, CA 90007

Dr. Kenneth O. Hartman 1
Hercules Aerospace Division
Hercules Incorporated
Allegany Ballistics Lab
P.O. Box 210
Cumberland, MD 21502

Dr. Joyce J. Kaufman 1
The Johns Hopkins University
Department of Chemistry
Baltimore, MD 21218

Dr. John K. Dienes 1
T-3, MS-216
Los Alamos National Lab
P.O. Box 1663
Los Alamos, NM 87544

Dr. H.P. Marshall 1
Dept. 52-35, Bldg. 204.2
Lockheed Missile & Space Co.
3251 Hanover Street
Palo Alto, CA 94304

Professor John Deutsch 1
MIT
Department of Chemistry
Cambridge, MA 02139

Professor Barry Kunz 1
College of Sciences & Arts
Department of PHysics
Michigan Technological Univ.
Houghton, MI 49931

Dr. R. Bernecker 1
Code R13
Naval Surface Weapons Center
White Oak
Silver Spring, MD 20910

Dr. C.S. Coffey 1
Naval Surface Weapons Center
Code R13
White Oak
Silver Spring, MD 20910

DISTRIBUTION LIST

	No. Copies
Dr. W. L. Elban Code R13 Naval Surface Weapons Center White Oak Silver Spring, MD 20910	1
Mr. K.J. Graham Naval Weapons Center Code 3835 China Lake, CA 93555	1
Dr. B. Junker Office of Naval Research Code 421 Arlington, VA 22217	1
Prof. H.A. Rabitz Department of Chemistry Princeton University Princeton, NH 08540	1
Dr. M. Farber Space Sciences, Inc. 135 West Maple Avenue Monrovia, CA 91016	1
Mr. M. Hill SRI International 333 Ravenswood Avenue Menlo Park, CA 94025	1
U.S. Army Research Office Engineering Division Box 12211 Research Triangle Park, NC 27709	1
U.S. Army Research Office Metallurgy & Materials Sci. Div. Box 12211 Research Triangle Park, NC 27709	1
Professor G.D. Duvall Washington State University Department of Physics Pullman, WA 99163	1


FIL
07